Multi-radio diversity in wireless networks

Allen Miu · Hari Balakrishnan · Can Emre Koksal

Abstract This paper describes the *Multi-Radio Diversity* (MRD) wireless system, which uses path diversity to improve loss resilience in wireless local area networks (WLANs). MRD coordinates wireless receptions among multiple radios to improve loss resilience in the face of path-dependent frame corruption over the radio. MRD incorporates two techniques to recover from bit errors and lower the loss rates observed by higher layers, without consuming much extra bandwidth. The first technique is *frame combining*, in which multiple, possibly erroneous, copies of a given frame are combined together in an attempt to recover the frame without retransmission. The second technique is a low-overhead retransmission scheme called *request-for-acknowledgment (RFA)*, which operates above the link layer and below the network layer to attempt to recover from frame combining failures. We present an analysis that determines how the parameters for these algorithms should be chosen.

We have designed and implemented MRD as a fully functional WLAN infrastructure based on 802.11a. We evaluate the MRD system under several different physical configurations, using both UDP and TCP, and measured throughput gains up to 3× over single radio communication schemes employing 802.11's autorate adaptation scheme.

Computer and Communication Sciences, EPFL, Switzerland.

A. Miu (✉) · H. Balakrishnan · C. E. Koksal
MIT Computer Science and Artificial Intelligence Laboratory,
The Stata Center, 32 Vassar Street, Cambridge, MA 02139, USA
e-mail: aklmiu@csail.mit.edu

H. Balakrishnan
e-mail: hari@csail.mit.edu

C. E. Koksal
e-mail: emre.koksal@epfl.ch

Keywords Path diversity · Packet combining · Frame combining · Bit error · Wireless LAN · Wireless networks · Performance

1 Introduction

This paper describes the design and implementation of the *Multi-Radio Diversity (MRD)* system, which reduces the loss rate and improves the throughput observed by transport protocols and applications running over wireless local area networks (WLANs). Our approach uses *path diversity*, relying on multiple access points (APs) covering a given area (for uplink diversity) and multiple radios on the user's device (for downlink diversity). The hypothesis underlying this system is as follows: because frame losses are often path-dependent (e.g., due to multi-path fading), location-dependent (e.g., due to noise), and statistically independent between different receiving radios, multiple radios that all receive versions of the same transmission may together be able to correctly recover a frame, even when any given individual radio is not.

Most current WLAN deployments (e.g., those based on 802.11 [6]) use one or more APs that relay packets to and from a WLAN client. Each AP operates independently and each WLAN client can communicate with only one AP at a time. Because the properties of a single path vary with time and can undergo severe deterioration, the result is that communication often suffers from high packet loss rates, long delays, and even outages. These, in turn, degrade the performance of protocols like TCP and applications like mobile Internet telephony, streaming audio/video, and games.

In MRD, different APs with overlapping coverage and listening on the same radio frequency provide alternate communication paths for each frame transmission from a given WLAN client, while multiple wireless cards on the WLAN

client achieve the same result for transmissions to the client. MRD coordinates packet receptions across the different radios to improve loss resilience against path-dependent bit corruption. The idea is simple: even when each individual reception of a data frame is erroneous, it might be possible to combine the different versions to recover the correct version of the frame. In MRD, the entity that performs this *frame combining* task is the *MRD Combiner (MRDC)*.

MRD's frame combining algorithm divides each frame into blocks. For each block, the algorithm assumes that at least one of the received copies of a frame (including any possible retransmissions) contains the correct bit values for that block. The algorithm then attempts to reconstruct the correct frame by trying every version received for each block. The process succeeds if a particular block combination passes the checksum embedded in the data frame, and fails once the search exhausts all possible block choices for each block. The computational complexity of this algorithm is exponential in the number of blocks for which different versions were received, which depends on the number of blocks in each frame. We show how to pick the block size and evaluate its performance using theoretical analysis and real-world experiments. This approach to frame combining is reminiscent of an old, well-studied idea called "retransmissions with memory" [13, 35], where retransmissions of erroneous frames are combined with the original transmission in an attempt to recover the correct version of the data. Our contribution is to generalize this idea using a block-based technique to incorporate the spatial dimension as well.

The MRDC can often recover a corrupt frame without requiring a retransmission from the client, but frame combining will not always succeed. MRD uses a lightweight retransmission scheme running above the WLAN link layer to further improve error recovery. At the sender, the *MRD Sender (MRDS)* buffers all frames that have not yet been acknowledged (or given up on), and retransmits any frame that it believes has not been successfully received by the MRDC (after frame combining). To prevent adverse interactions caused by ARQ schemes at two different layers, MRD turns off link-layer retransmissions altogether. To keep overhead low and to react quickly to channel contention, however, MRD uses two techniques: first, it retains 802.11's synchronous ACK mechanism, with the MRDS clearing frames thus acknowledged from its retransmission buffer. But because some frames can only be recovered after frame combining, and because the MRDC does not know whether any given link-layer ACK reached the MRDS, MRD uses a feedback protocol between the MRDC and MRDS. This protocol is designed to have low overhead, using a *request-for-ACK (RFA)* technique rather than traditional ACKs or NACKs. With RFA, the MRDS explicitly requests an ACK from the MRDC for certain frames, and decides whether and when to retransmit frames based on this feedback.

A noteworthy aspect of MRD is that it achieves significant improvements in loss rates while consuming only a small amount of additional bandwidth. As a result, it complements both automatic repeat request (ARQ) and rate adaptation [1, 10, 22], two common error-control techniques used in contemporary WLANs. ARQ-based retransmissions work well when the duration of channel degradation is short. But when the channel's quality deteriorates for a long period, link-layer retransmissions triggered by a missing link-layer ACK become ineffective and wasteful. Rate adaptation, on the other hand, can work well even when the wireless channel experiences severe deterioration. However, efficient rate adaptation is difficult to achieve when channel conditions vary quickly and unpredictably, as is the case in many real-world WLANs, particularly when users are mobile.

Sections 2 through 5 of this paper detail the different contributions of this paper: the MRD architecture, the frame combining algorithm and its theoretical analysis, the RFA scheme, and the MRD modifications to the 802.11 WLAN rate adaptation schemes. Section 6 describes our fully functional 802.11a/b/g-based Linux implementation of MRD. Section 7 presents the results of several experiments conducted over an in-building 802.11a-based testbed at MIT's Computer Science and Artificial Intelligence Laboratory. Experiments that experienced a high channel variability (e.g., a mobile WLAN client that moved over a relatively small area of about three square meters) show throughput improvements of up to $3\times$ compared to contemporary 802.11a with "autorate adaptation" [1].

2 Multi-radio diversity architecture

For ease of exposition, we describe the MRD architecture in the context of uplink transmissions from the client to the WLAN infrastructure. The same architecture can be used when the MRD radios are co-located on the same device (either in a single AP or on the WLAN client).

Figure 1 shows the MRD system architecture. Each AP in the WLAN infrastructure offers a different physical commu-
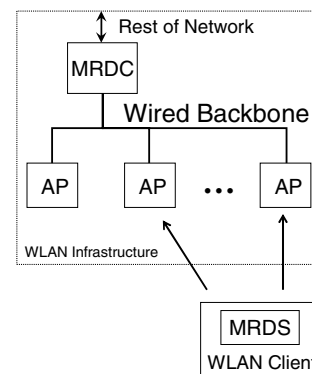

Fig. 1 MRD system architecture

nication path between the client and the rest of the network. We configure the APs to listen on the same radio frequency so they can each receive a copy of the client's uplink transmission. The AP forwards all frames—including those that are corrupted—to the MRD Combiner (MRDC), which filters redundant data frames received by multiple radios and invokes the frame combining procedure when needed. The MRDC maintains a packet buffer to deliver packets in-order to the rest of the network.

At the WLAN client sender, the MRDS handles data transmissions and retransmissions. The MRDS operates in between the link-layer and the IP network layer. It keeps track of unacknowledged transmissions and schedules their retransmissions when it believes that the MRDC has failed to receive a clean copy of the transmitted frame from any of the APs and has failed to correct their errors via frame combining. The MRDS uses the RFA protocol to obtain the results of the frame combining procedure from the MRDC.

The MRD WLAN architecture does not preclude cellular frequency reuse. Frequency reuse is a common method to increase network capacity, which requires APs in neighboring cells to operate in different radio frequencies. In MRD, the APs that are not explicitly associated with the client need only listen for uplink transmissions *passively*. Thus, one strategy to achieve frequency reuse is to install *passive* radios in addition to the regular, *active* radio at each AP.[1] The client associates with the active radio at each AP, which serves the regular function of transmitting management and control frames to the WLAN client, while the passive radios are configured to listen on the neighbors' radio frequencies. Because the passive radios never transmit a frame, they do not create any interference in the network. If installing multiple radios on a single AP is not possible, an operator can install additional passive access points in the network. As the costs of APs continue to decline, this approach is a viable way to add path diversity (for uplink communication) in WLANs.

MRD assumes that there is sufficient bandwidth in the wired backbone to handle the additional traffic generated by the passive APs. This assumption is reasonable because the number of APs within reception range of a transmitter is usually low and the speed of the wired backbone[2] is usually one or two orders of magnitude higher than the wireless link.

MRD does not affect the functions of handoff and security in a WLAN. As in the conventional wireless LAN, the WLAN client would associate with and perform handoffs between different active APs. Existing WLAN security standards such as WEP [6], 802.1x [7], and WPA/802.11i [4]

---

[1] In fact, companies have begun selling radio chipsets that can process and decode transmissions from multiple channels simultaneously (see, e.g., [3]).

[2] In the downlink direction, the "backbone" is the internal bus interconnecting the wireless interfaces within a client.

handle encryption/decryption and other security functions in software and are easily implemented in the MRDS and the MRDC, assuming that the MRDC can establish a secure trust relationship with each MRD radio (AP) over the network.

3 Frame combining

We now describe how MRD recovers error-free versions of corrupted data frames using frame combining and analyze its performance. One approach is to run a simple linear time algorithm that attempts to correct bit errors by selecting the majority bit value between three or more frames [15]. But this approach requires at least three copies of the same transmitted frame, which may not be available (without a retransmission) if only two MRD radios are within receiving range of the sender. Therefore, we develop and analyze a block-based frame combining scheme that can work even when only two copies are available.

Suppose two copies of the same transmitted frame of size S bits are received at two different receivers. If any of the data frames passes the link-layer cyclic redundancy checksum (CRC) check, the MRDC decodes it as the transmitted frame and forwards it—we term this step *soft selection*. Otherwise, the MRDC runs the block-based combining algorithm to recover the packet. Block-based frame combining works by first subdividing both frames into blocks, and then reconstructing the frame by assembling the blocks selected from each received frame of the transmitted packet. The process succeeds if a block combination passes the CRC embedded in the data frame, and fails once the search exhausts all possible block combinations.

For the two-frame case, the block combining steps are:

1. The input to the algorithm is two frames, $f = \{\mathcal{A}, \mathcal{B}\}$, of size S bits each, divided into N_B blocks $X = \{X_1^f, X_2^f, \ldots, X_{N_B}^f\}$. Let $\Delta = |\{i | X_i^{\mathcal{A}} \oplus X_i^{\mathcal{B}} \neq 0\}|$ (i.e., the number of blocks that do not have matching bit values). All matching blocks from $\mathcal{A}$ and $\mathcal{B}$ are retained unmodified.

2. Assemble a combined frame that contains $X' = \{X_1^{f'}, X_2^{f'}, \ldots, X_{N_B}^{f'}\}$ blocks from either frame $\mathcal{A}$ or $\mathcal{B}$. Each iteration of this step generates a new combined frame by replacing $X_i^{f'}$ with either $X_i^{\mathcal{A}}$ or $X_i^{\mathcal{B}}$ for each i where $X_i^{\mathcal{A}} \oplus X_i^{\mathcal{B}} \neq 0$.

3. If either of the CRC value embedded in frames $\mathcal{A}$ or $\mathcal{B}$ matches the CRC value computed over X', return the combined frame containing X'. Otherwise, repeat step 2 until all possible combinations of X' have been tried. If none of the block combinations X' passes the CRC check, declare a frame combining failure.

There are many ways of dividing a frame into blocks. For simplicity, we divide each frame such that blocks

(a) Receiver-pair frame loss rates   (b) Bit-error location histogram   (c) Bit-error conditional probabilities
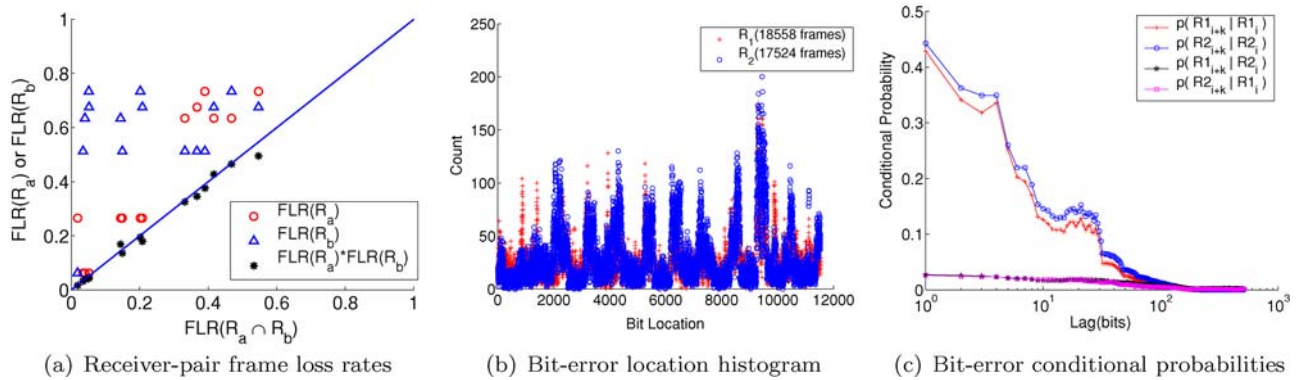
Fig. 2 Error analysis. Figure 2(a) suggests that frame losses occur independently between any pair of simultaneous receivers in our experiment. Figure 2(b) shows that the bit-errors are clustered in a regular pattern within a frame. The number in the legend indicates the number of corrupt frames received at each node. The conditional probabilities in Fig. 2(c) suggest that bit-errors occur in bursts within a frame but bit-errors between frames received at different locations have low correlation

$X_1^f, X_2^f, \ldots, X_{N_B-1}^f$ contain B bits and the size of the last block $|X_{N_B}^f|$ is $\leqslant B$. Thus, $N_B = \lceil S/B \rceil$.

When the block-based frame combining algorithm declares a failure, the MRDC can save the corrupt frames for possible frame combining (using either bit-majority or block-based combining) with any subsequent retransmissions of the frame. In our current implementation, the MRDC saves only one of the corrupt frames and apply block-based combining to two corrupt frames at a time. Note also that the algorithm generalizes easily to more than two concurrent receptions of the same frame.

The block-based frame combining algorithm is simple but its running time is exponential in Δ, the number of differing blocks. With two copies, it needs up to 2^Δ CRC check operations to identify the correct combination. Since $\Delta \leq N_B$, one way to bound the number of CRC checks is to reduce N_B by increasing B. Inevitably, the frame combining failure probability will increase as the likelihood of simultaneous block errors increases with B. We analyze this tradeoff next.

3.1 Frame combining failure analysis

We analyze how the frame combining failure probability, p_f, varies with N_B under a burst bit-error channel model parameterized by a burst length b. p_f is the fraction of frames that cannot be corrected with combining out of those that could not be corrected by the soft selection in the first place. To find the overall retransmission probability, we assume that each receiver observes independent losses, and multiply p_f with the independent frame loss rates (*FLR*) at each receiver $FLR(R_a) \times FLR(R_b)$ (i.e., the probability that the frame goes uncorrected by soft selection). Indeed, loss independence may not be valid under certain conditions, such as losses caused by interfering signals generated from an active source (e.g., a microwave oven).

However, for losses that are path-dependent, losses tend to occur independently among different receivers. We ran a broadcast experiment involving six simultaneous 802.11a receivers, distributed at various locations on the same floor of an indoor lab space. The sender broadcasted 500,000 1500-byte UDP frames, each tagged with an unique sequence number, at saturation rate. We then take each pairwise combination of the six receivers and for each receiver pair, we computed the *FLR* at R_a and R_b, and their simultaneous loss rate ($FLR(R_a \cap R_b)$), i.e., the rate at which both receivers simultaneously observe a loss of the same transmitted frame.

Figure 2(a) plots the individual *FLR* on the y-axis for R_a (circle) and R_b (triangle) vs. the simultaneous *FLR* for the R_a and R_b pair on the x-axis.[3] The plot shows that the individual *FLR* are greater than the simultaneous *FLR*, which suggests losses are not completely correlated between any two receivers.

To test for loss independence, we plot the product of the individual *FLR*s (star) vs. simultaneous *FLR*. The plot shows that the product values lie roughly on the $y = x$ line. This indicates that $FLR(R_a)FLR(R_b) \approx FLR(R_a \cap R_b)$, which suggests that losses are largely independent at each receiver in our experiment. Another similar wireless measurement study observes loss independence among simultaneous receivers as well [38]. In Section 7, we conduct more exhaustive experiments that show that MRD works well in practice, indirectly further validating the independence hypothesis.

Using the same experiment, we validate the assumption that bit-errors occur in bursts by analyzing the bit-error patterns of over 36,000 corrupt data frames for a specific pair of receivers R_1 and R_2. Figure 2(b) plots a histogram of the bit-error locations, which shows that the error distribution is uneven, often clustered within 100–200 bits, spaced

---

[3] Circles and triangles that lie on the same x-axis value belong to one R_a and R_b receiver-pair. There are $\binom{6}{2} = 15$ receiver pairs in total.

Fig. 3 The PMF for the number of bit-errors for two different placements of the receiver pair
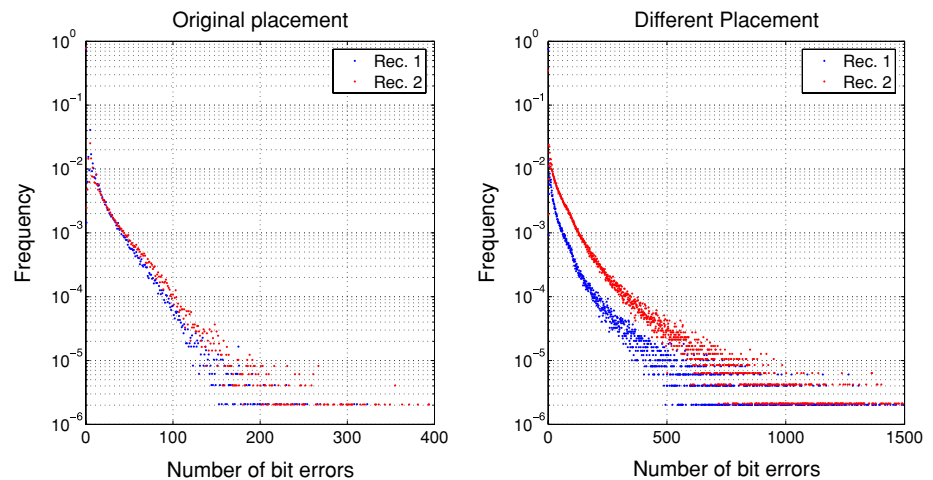
between 800–1200 bit positions apart. At the 48 Mbps bit-rate, 802.11a employs QAM-64 modulation at 2/3 coding rate. This burst pattern is also observed in other node placements on our testbed and also in another 802.11b testbed deployed in an industrial environment [40].

Next, we examine how bit errors are correlated between different receivers for the same frame transmission. Let $R1_i$ and $R2_i$ represent the event that the ith bit of the transmitted frame is received in error by receivers $R1$ and $R2$ respectively. Then, $P(R1_{i+k}|R1_i)$ and $P(R2_{i+k}|R2_i)$, for $k > 0$, represents the "auto-conditional loss probability" that the $(i + k)$th bit is corrupt, given that the ith bit is corrupt in the same frame. Similarly, we use $P(R2_{i+k}|R1_i)$ and $P(R1_{i+k}|R2_i)$ to represent the "cross-conditional loss probability" that the $(i + k)$th bit is corrupt, given that the ith bit is corrupt in the frame received by the alternate receiver.

Figure 2(c) shows the auto-conditional and cross-conditional bit-error probabilities for all the corrupt frames. The cross-conditional probabilities remain flat even at the bit level. The cross-conditional bit-error probabilities for $k < 100$ are much lower than their counterpart auto-conditional probabilities, which suggests that bit-errors rarely occur simultaneously at nearby locations between two frames received at different physical locations. In contrast, the auto-conditional error probability at the bit level increases dramatically at small k (< 100). The increased auto-conditional probability corresponds to the burst bit-error behavior and is most likely related to the clustered bit-error patterns shown in Fig. 2(b).

We believe that the periodic and burst nature of bit-errors observed in our experiments is due to the orthogonal frequency division multiplexing (OFDM) scheme employed in 802.11a. In this scheme, 52 separate sub-carriers are used to provide separate wireless pathways for sending the information in parallel. Four of them are used for control, and each of the remaining 48 sub-channels carries upto 1 Mbps summing to 48 Mbps. We believe that the non-uniformity of the losses

is because different parts of a frame are carried by different channels, and the periodicity of bit-errors arises because the same set of data bits in each frame are consistently assigned to the same sub-channel. Indeed, QAM-64 implies that there are 6 bits/symbol on each sub-carrier and hence the bunching of $6 \times 48 \times 2/3 = 192$ data bits per OFDM symbol is consistent with this hypothesis. Also, the 800–1200 bit spacing of the peaks may be caused by the time-varying nature of the channel between the stationary transmitter and receivers.

These experimental observations motivated us to develop an analytic model that allows us to examine how p_f is affected by the bit-error burstiness in the communication channel. In our model, we assume that bit-errors occur in bursts of $b \geqslant 1$ bits. Moreover, we assume that these sequences of consecutive b bit-errors are spread uniformly over the frame. Thus, if there occur d such sequences in a given frame, then it means there are a total of bd bit-errors in that frame. We neglect the effect of two individual error sequences starting within b bits of each other.

Let $D_{b,i}$ represent the number of b-bit sequences with errors in a given frame received at receiver R_i. Then,

$$P(D_{b,i} = d | D_{b,i} > 0) = \eta \sum_{d'=(d-1)b+1}^{db} P(D_i = d'). \quad (1)$$

where $\eta = (1 - P(D_i = 0))^{-1}$ and $P(D_i = d')$ is the probability that a frame received by R_i contains d' bit-errors.[4] We obtain the distribution of number of bit-errors empirically. Figure 3 shows the probability mass function of the number of bit-errors for two broadcast experiments using different node placements. We found empirically that given that a frame contains bit-errors, $P(D_i = d')$ decays almost exponentially, i.e., as $e^{-\alpha d}$ where $\alpha \approx 0.01$—0.05.

---

[4] Note that b may not divide into d' evenly so the summation in 1 includes all d' for a given $D_{b,i}$ such that $D_{b,i} = \lceil d'/b \rceil$.

In our model, we kept the average number of bit-errors per packet fixed (independent of b) and b controls only the burst size. This model of fixed sized bursts of error implies that the auto-conditional bit-error probability distribution is a step function with a jump at b. Even though the step function only approximates the real auto-conditional bit-error probability distribution shown in Fig. 2(c), it encompasses certain flavors of wireless channels where losses occur in bursts.

Let us denote the set of blocks with errors at receiver R_i by $\mathcal{N}_i$. Then $|\mathcal{N}_1 \cap \mathcal{N}_2|$ represents the set of blocks that contain simultaneous errors at both R_1 and R_2.

To derive the frame combining failure probability, p_f, we make a simplifying assumption that ignores the possibility that a sequence can spread over more than one block. This assumption is reasonable when $b \ll B$, which is likely to be the case in reality.

If the sequences of bit-errors are uniformly distributed over the frame, the probability of getting at least d simultaneous block errors, conditioned on the event that receiver R_i receives a frame with d_i trains of burst errors is at most

$$\begin{aligned}
&P(|\mathcal{N}_1 \cap \mathcal{N}_2| \geqslant d | D_{b,1} = d_1, D_{b,2} = d_2) \\
&\leqslant \frac{\binom{N_B}{d}\binom{N_B+d_1-d-1}{d_1-d}\binom{N_B+d_2-d-1}{d_2-d}}{\binom{N_B+d_1-1}{d_1}\binom{N_B+d_2-1}{d_2}},
\end{aligned} \quad (2)$$

for $d < \min\{d_1, d_2, N_B\}$. The analogy with a ball placement problem is as follows. We have d_1 red and d_2 blue balls to be placed in a total of N_B bins randomly. We evaluate the probability that at least d bins contain both red and blue balls. First, we place d red balls and d blue balls in a given combination of d bins so that each bin contains exactly one red and one blue ball. Then we distribute the remaining $d_1 - d$ red and $d_2 - d$ blue balls randomly in all possible N_B bins. We end up with an upper bound because the expression counts invalid combinations that place more than $\lceil B/b \rceil$ sequences of b-bit errors within a block, which cannot happen in reality.

Because a frame combining failure occurs when $d \geqslant 1$, the conditional frame combining failure probability is simply

$$p_f(d_1, d_2) = P(|\mathcal{N}_1 \cap \mathcal{N}_2| \geqslant 1 | D_{b,1} = d_1, D_{b,2} = d_2). \quad (3)$$

The upper bound on the unconditional probability of combining failure is

$$p_f \leqslant \sum_{d_1=1}^{\lfloor S/b \rfloor} \sum_{d_2=1}^{\lfloor S/b \rfloor} p_f(d_1, d_2) \prod_{i=1}^{2} P(D_{b,i} = d_i | D_{b,i} > 0). \quad (4)$$

and can be computed using Expressions (1) to (4). Note that this bound is tight since the a priori probabilities for the d_i values exceeding B/b for typical values of b and B are very
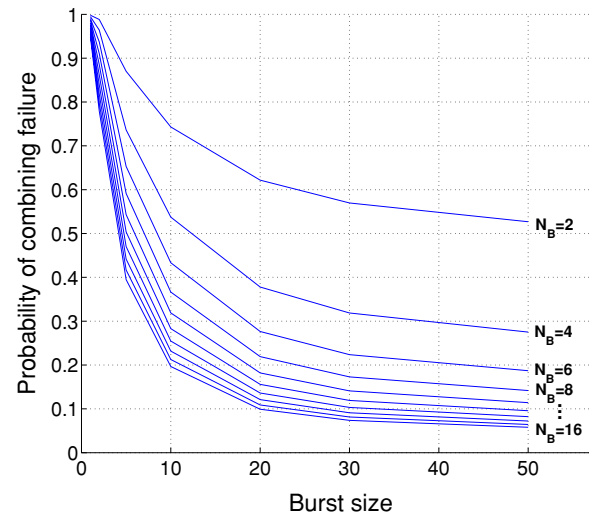

Fig. 4 The upper bound on p_f as a function of the burst size, b. From top to bottom, the curves are plotted for the span of values of number of blocks, $N_B = 2, 4, 6, 8, 10, 12, 14$ and 16

small. Thus in the summation in (4), the weights associated with the a posteriori probabilities of invalid events of placing more than $\lceil B/b \rceil$ sequences of b-bit errors within a block are very small.

Figure 4 plots the upper bound on p_f as a function of the burst size b for several values of the block size, N_B. If the bit-errors are uniform ($b = 1$), p_f remains high (≈ 1) regardless of N_B. However, the auto-conditional probabilities in Fig. 2(c) suggests that bit-errors indeed occur in bursts. In this case, we expect p_f to decrease with increasing N_B. As N_B gets larger, the difference between the two curves for a given b becomes very small, which suggests that increasing N_B beyond a certain point does not yield much improvement. Thus, we lose little performance by fixing N_B to some small value (say, 6–10) in order to bound complexity. Because p_f is a highly convex function of b, we expect the performance of frame combining to be sensitive with respect to the changes in the burstiness of the bit-errors in the channel. Moreover, the performance of frame combining will improve as the available computational power increases.

3.2 False positives

We now comment on the possibility of false positives in the combining process caused by repeated trials for the CRC to check with distinct frames. In essence, the CRC is an n-bit parity check field that detects any $k < n$ bit errors and misses detection with probability 2^{-n} when $k \geqslant n$. Thus, if a 32-bit CRC is used, as in 802.11, any number of bit errors <32 is detected. Moreover, the probability that any randomly produced frame will check the CRC is 2^{-32}, which implies that it is almost impossible for a random bit error pattern to go

undetected even if a frame contains more than 31 erroneous bits.

Now, with frame combining, even though a single check leading to a false positive is highly unlikely, if we try it repeatedly many times, we may end up getting a false positive. Indeed, if the number of differing blocks in two frames is Δ, the number of swaps (and the number of tests for the CRC to check) is 2^Δ. For independently produced 2^Δ frames, the false positive probability is

$$P(\text{false positive}) = 1 - (1 - 2^{-32})^{2^\Delta}$$
$$\approx 1 - \exp(-2^{\Delta-32}).$$

Thus, if $E\left[2^\Delta\right]$ is close to 2^{32}, it is likely that the combining procedure leads to false positives. Even if the available computational power can perform 2^{32} CRC tests, we pick a block size that is sufficiently large (i.e., N_B is sufficiently small) so that, even in the worst case, we do not perform too many CRC checks. Hence, we guarantee by design that $2^\Delta \ll 2^{32}$ and keep the false positive probability sufficiently small. Our implementation uses $N_B = 6$. Furthermore, most higher layer protocols such as UDP and TCP uses an extra 32-bit CRC to provide an end-to-end data integrity check. Thus, the probability of forwarding to the application an erroneous packet with a false CRC is minuscule in practice.

4 Retransmissions with RFA

MRD disables link-layer retransmissions to allow the MRDC to recover packets that the active radios receive in error. The MRDS retransmits frames that the MRDC fails to recover with soft selection or frame combining (i.e., a frame recovery failure). To facilitate these retransmissions, the MRDS uses the *request-for-ACK* (RFA) protocol to obtain the status (success or failure) of each frame transmission.

4.1 Design of RFA

RFA operates in between the link-layer and the network layer, but uses the link-layer synchronous ACKs that is implemented in most WLANs such as 802.11. A synchronous ACK is a link-layer control packet that is sent by the active radio (see Section 2) immediately after it successfully receives a data frame. After each frame transmission, the MRDS checks the link-layer transmission status. A success implies that the active radio has received the transmission correctly, so the MRDS can proceed to transmit the next available packet. A failure implies either a corrupt link-layer ACK or a corrupt data transmission. In the former case, the MRDC simply forwards the correctly received data packet or buffers it in the reorder buffer (explained below in Section 4.3). In the latter case, the MRDC may recover the frame loss using soft selection or frame combining. If the recovery is unsuccessful, the MRDC saves the corrupt frames for possible frame combining with any subsequent retransmissions of the frame.

In either case, the MRDC always knows the final status of each frame transmission. Thus, when the MRDS fails to receive a link-layer ACK, it issues a "request-for-ACK" frame to the MRDC to obtain an *MRD acknowledgment* (MRD-ACK), which contains the authoritative status of the transmission. The MRDS needs to explicitly issue an RFA because only the MRDS knows which frames are ACKed by the link-layer.[5] To save overhead, the MRDS signals a RFA by setting a flag in the frame header of subsequent data transmissions. We explain the implementation details of RFA in Section 6.2.

The MRDS buffers the frame that fails to receive a link-layer ACK for later retransmission and schedules the next available frame for transmission. The subsequent transmissions keep the wireless channel utilized while the MRDS waits for the frame recovery results from the MRDC, which can take many milliseconds. To limit the size of the retransmission buffer, the MRDS may transmit up to N different frames from the first unacknowledged one. The MRDS removes a frame from the transmission buffer after K unsuccessful retransmission attempts. The MRDS schedules a retransmission if the MRD-ACK indicates a frame recovery failure. If the MRDS never receives an ACK from the MRDC, the MRDS will schedule all outstanding unacknowledged packets for retransmission after a timeout, T_s. Our current implementation uses a static timeout value of 90 ms.

There are two reasons why we chose to use the link-layer ACK, instead of eliminating it and letting MRDS and MRDC handle retransmissions using a standard automatic repeat request (ARQ) protocol that operates strictly above the link-layer. First, the synchronous ACKs are necessary for carrier-sense multiple access (CSMA) to operate properly. CSMA uses a randomized backoff window and relies on the absence of the synchronous ACK packet to detect contention and adjust the backoff window *after each frame transmission*. Because we allow transmissions to continue while the MRDS waits for an MRD-ACK from the MRDC, it is important to preserve the underlying CSMA channel access mechanism.[6]

Second, the wireless medium is already reserved for the transmission of synchronous ACKs in 802.11. They are designed (by means of a smaller data-to-ACK frame spacing time) to not collide with data transmissions from another nearby source. In contrast, the acknowledgments from the

---

[5] In our implementation, the MRDC also uses the RFA signal to help it flush the reorder buffer.

[6] It is conceivable to use some other channel access schemes besides CSMA (e.g., TDMA). Doing that would require introducing a major modification to the medium access control (MAC) layer of 802.11.

MRDC are asynchronous and must therefore contend for the channel and suffer potential collisions. Thus, it is a good idea to avoid sending asynchronous ACKs as much as possible, especially during times when the channel quality is good and link-layer losses are low.

4.2 Delaying acknowledgments

To reduce the number of MRD-ACKs sent to the sender, the MRDC delays the return of an MRD-ACK frame by up to D frame-transmission times, where $0 < D < N$. D should be greater than 0 because the MRDC needs time to gather corrupt frame copies from the MRD radios and perform frame combining. A smaller D value would cause the system to incur higher overhead as the MRDC would send MRD-ACKs more often. A higher D reduces overhead, but can cause larger transmission delay when the frame requires retransmission. In practice, the added delay is of little concern to higher layer transport protocols and most multimedia applications because D is usually set to a few frame transmission times, on the order of a few milliseconds. If $D > 1$, the MRDC could process multiple frames before returning an MRD-ACK to the MRDS. We expand the MRD-ACK packet with a bit-vector to indicate the final status of several packets at once, instead of spreading the acknowledgment across several different MRD-ACK frames.

4.3 In-order packet delivery

The MRDC maintains a reorder buffer to ensure that packets are forwarded in-order to the rest of the network. When a frame requires retransmission, the MRDC inserts all subsequently transmitted frames into the reorder buffer until the missing frame has been successfully recovered or has been given up on.

There are many applications, such as audio and video streaming, which are sensitive to packet delays but do not require in-order packet delivery. To cater to these applications, we can mark specific frames for out-of-order delivery. Such frames can avoid being delayed inside the reorder buffer. Our current implementation does not include this feature but it could be added easily.

5 Rate adaptation in MRD

Rate adaptation (or "autorate") works well when the communication channel severely deteriorates and should be used in MRD when soft selection and frame combining can no longer recover frame losses effectively. Traditional autorate algorithms try to maximize throughput by using loss or signal strength information observed by a single receiver. Current autorate algorithms behave sub-optimally under MRD

```
INIT()
    stable ← 0
    numtx ← 0
    numtxok ← 0

TxCallback()
    numtx ← numtx + 1
    if (txsuccess)
        numtxok ← numtxok + 1

RateAdjust()
    if ((numtx > 0 and numtxok == 0) or
        (numtx ⩾ 10 and numtxok/numtx < 𝒟))
        if (bitrate > 0)
            bitrate ← bitrate − 1
            INIT()
    elseif (numtx ⩾ 10 and numtxok/numtx > 0.90)
        stable ← stable + 1
        if (stable ⩾ S and bitrate < MAX_BITRATE)
            bitrate ← bitrate + 1
            INIT()
    else
        stable ← stable + 1
```

Fig. 5 Pseudo-code of the MADWiFi autorate algorithm

because they do not use information observed at *all* of the diversity radios that are within range of the sender.

The interaction between rate adaptation and MRD error control is an interesting open topic. Here, we present some simple modifications to an existing rate adaptation algorithm. Although these modifications may not necessarily yield an optimal algorithm for MRD, we found them to work well in our experiments.

Our testbed implementation is based on 802.11 interfaces that use the Atheros 5212 chipset, which are driven by the Multiband Atheros Driver[7] for WiFi (MADWiFi) [1]. The MADWiFi driver implements an autorate algorithm that adjusts bit-rates based on the observed link-layer frame loss rate. Due to the popularity of MADWiFi, the MADWiFi autorate algorithm is becoming a *de facto* benchmark. Its performance has been studied extensively in [10] and [22] and is shown to outperform the Auto Rate Fallback (ARF) algorithm that is implemented in many 802.11 interfaces on the market. We use the MADWiFi autorate algorithm as the basis of discussion, but the general ideas in this section can be applied to many other loss-based autorate algorithms.

Figure 5 provides a pseudo-code of the MADWiFi autorate algorithm. In our notation, $bitrate$ is an integer with a range [0..MAX_BITRATE], which represents the set of discrete bit-rates available to the sender. There eight discrete bit-rates in 802.11a (6, 9, 12, 18, 24, 36, 48, 54 Mbps).

---

[7] pci: v.0.8.6.1, hal: v.0.9.12.5, wlan: v.0.7.3.2.

```
MRDCALLBACK()
    numtxok ←
        numtxok + min(numacked, numtx − numtxok)
```

Fig. 6 A procedure that helps autorate maintain a better estimate of *numtxok* in MRD

The MADWiFi algorithm starts by calling INIT() and invokes TXCALLBACK() to update the *numtx* and *numtxok* counters after each frame transmission. The algorithm invokes RATEADJUST() once every T seconds. If the frame delivery rate is above 90% for at least S number of successive periods, increase the bit-rate. If it falls below a minimum delivery threshold $\mathcal{D}$, decrease the bit-rate.

The original algorithm adjusts the *numtxok* counter based on link-layer feedback. This approach can lead to an understated *numtxok* value in MRD because the MRDC can recover many frame transmissions using soft selection or frame combining. To fix this problem, we add the routine listed in Fig. 6 to the MADWiFi autorate algorithm.

The MRDS invokes MRDCALLBACK() whenever it receives an MRD-ACK. *numacked* is the number of frames (unacknowledged by the link-layer) reported in the MRD-ACK that have a successful delivery status at the MRDC and is added to *numtxok*. Thus, MRDCALLBACK helps the autorate algorithm maintain a correct estimate for *numtxok* as long as it receives some MRD-ACKs. Even if an MRD-ACK packet is dropped for some reason, the *numtxok* can still be adjusted to the correct value by the subsequent MRD-ACKs because the MRD-ACKs cumulate the ACK bit vector for any unacknowledged packet. But because *numtxok* can be adjusted only upon receiving an MRD-ACK packet, long delays between MRD-ACK receptions can still cause an understatement in the *numtxok* value. This is not usually a problem in practice because 1) MRD-ACKs are always transmitted at the lowest (most robust) bit-rate to minimize loss, and 2) we set a low delay threshold (16 ms in our implementation) for transmitting MRD-ACKs.

Another problem with the original MADWiFi algorithm is that the default minimum delivery threshold $\mathcal{D}$ is fixed at 50%, which, as noted in [10], is inefficient for 802.11a/g. Let $\mathcal{D}_r$ and R_r be the expected delivery rate and effective throughput[8] using bit-rate r. Then, the throughput achieved by the lower bit-rate is the same as the current bit-rate if $\mathcal{D}_{r-1} \times R_{r-1} = \mathcal{D}_r \times R_r$.

R_{r-1} and R_r are known values and in general, $\mathcal{D}_{r-1} > \mathcal{D}_r$ because lower bit-rates are more robust against loss. To minimize loss, we set $\mathcal{D}_{r-1} = 1$. Thus, the ideal minimum

---

[8] The effective throughput is lower than the bit-rate because of link-layer overhead.

Table 1 The mean and median throughput of one second non-overlapping window samples across all five trials in each experiment

Scheme	Mean (Mbps)	Median (Mbps)
Slow R1	4.95	4.68
Fast R1	8.25	7.07
Slow MRD-R1	19.29	19.85
Fast MRD-R1	18.76	19.06

delivery threshold for bit-rate r is $\mathcal{D}_r = R_{r-1}/R_r$, the ratio of the effective throughput at the lower and higher rates.

In 802.11a, the typical value for R_{r-1}/R_r varies from 0.6 to 0.8. Thus, fixing $\mathcal{D} = 0.5$ is too low and causes the transmitter to maintain the current bit-rate even though its delivery rate is well below the break even point. We modified the MADWiFi algorithm to lower bit-rates according to the proper break-even ratios in our implementation.

Finally, the default values for T and S ($T = 1$ second and $S = 10$) cause the MADWiFi algorithm react too slowly to rapid changes in the channel. Instead, we set lower values $T = 0.5$ and $S = 2$ to improve its responsiveness. We ran an experiment with a high channel variability (by using mobile transmitter, described in Section 7.1) to compare the performance of the algorithm using different parameter values. Table 1 shows that the modified parameter values (Fast) helped increase throughput by about 67% over the default parameter values (Slow) for the single radio experiments using R1.

Intriguingly, the performance difference between Slow MRD and Fast MRD is negligible, suggesting that MRD is relatively insensitive to the particular parameter values chosen for rate adaptation. Being able to perform consistently under different parameter values is useful, because determining the optimal parameter values for any kind of adaptive algorithm is often difficult in practice.

6 Implementation

This section describes the implementation of the MRD system and the RFA protocol in detail.

6.1 System implementation

We implemented the MRD system using commodity contemporary Pentium class PCs running Linux Kernel 2.4.20 and 802.11a/b/g wireless interfaces (Netgear WAG311 PCI-card on the PC and Proxim 8480 PC-card on the laptop) based on the Atheros 5212 chipset. We modified the MADWiFi driver to implement the MRDS component for 802.11a/b/g WLAN clients.

As described before, the primary function of the MRDS is to schedule retransmissions. To handle retransmissions within the driver software, we disable the wireless interface

from retransmitting packets by setting the retry limit to zero. During our experimental evaluation, we discovered that doing so caused the distribution of frame inter-transmission times to peak at the nominal packet transmission time, despite many transmission losses. In other words, setting a zero retry limit also disabled exponential backoff in the 802.11 interface. It turns out this is the behavior mandated by the original 802.11 standard [6]: the contention window should reset to the lowest value after a packet reaches its retransmission limit.

Consequently, our current MRD implementation does not include CSMA exponential backoff. However, future releases [5] of the MADWiFi driver [1] will include software support for 802.11e [18], which includes a software API to allow the driver to modify the contention window size. Meanwhile, we have disabled exponential backoff in *all* of our experiments to make fair performance comparison between the 802.11 standard and our MRD-enhanced 802.11 system.

We used desktop PCs equipped with 802.11 wireless interfaces as access points. One AP acts as the active radio and is configured to run in the MADWiFi's "AP Master" mode. The passive radios are configured to run in MADWiFi's "Monitor" mode. On each of the APs, we run a user-level daemon to capture data frames from the wireless interface and forward them over a wired backbone (100 Mbps Ethernet in our experiments) to the MRDC running on another PC.

For increased efficiency, the AP daemon performs the CTX header checksum (see the next section) and drops frames that cannot be used for frame combining (i.e., those frames with a corrupt header). Because the RFA protocol does not require the client to acknowledge the receipt of an MRD-ACK, the AP daemon prepends the target client's MAC address in the MRD-ACK payload and transmits each MRD-ACK as a broadcast frame. Broadcasts saves the transmission of link-layer ACK frames in unicast and the benefit is much larger than the cost of expanding the size of the MRD-ACK payload. In our actual implementation, the AP

daemon writes the target client's 6-byte MAC address in the source address field of the 802.11 header, thus saving us from expanding the MRD-ACK payload at all. We transmit the MRD-ACK packet at the lowest data rate (6 Mbps for 802.11a/g and 1 Mbps for 802.11b) for robust delivery.

Because the CRC computation is the bottleneck of the frame combining process, it is important to make it as efficient as possible. The MRDC currently implements a widely-used 8-bit table lookup algorithm to compute the 32-bit CRC checksum of a combined frame. Although the algorithm is simple, it is rather inefficient to process the entire frame to compute a new CRC value when the bit values for only a small portion of the frame changes during each iteration of the frame combining algorithm. Although not implemented, there are incremental CRC algorithms that can reduce the running time of repeated CRC checks by over an order of magnitude [12, 34]. The computation savings can be used by the frame combining algorithm to improve frame combining success rate through using smaller block sizes.

We implemented the MRDC as a user-level daemon running on a 1.5 GHz Pentium 4 PC. Implementing the MRDC as a user-level daemon facilies debugging and running diagnostics. It forwards clean or corrected packets to the tunneling driver so that the Linux kernel can forward the packet using `iptables`.

6.2 Implementation of RFA

Figure 7(a) shows the headers used by RFA. For every data frame transmission, the MRDS inserts a 7-byte Combiner Transmit (CTX) header prepends the payload of the MAC-layer frame. The CTX header contains a *ctrl* field, which uses 4 bits to indicate the number of attempted transmissions (*ntx*) for the current data frame, 1 *rfa* bit to indicate that the sender has pending unacknowledged frames and is requesting for acknowledgment, and 3 unused bits reserved for future options such as out-of-order delivery. The 1-byte *seq* field
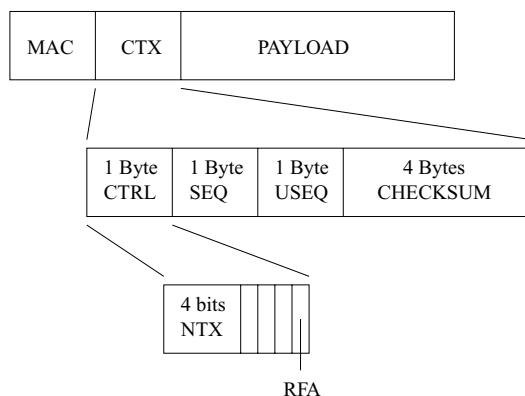
(a) Headers in the transmitted data frame

(b) MRD-ACK Packet

Fig. 7 MRD-ACK control information

labels the sequence number of the data frame, while *useq* labels the oldest transmitted data frame in the MRDS buffer that has not been acknowledged by the MRDC. When frame *useq* exceeds its retransmission limit, the MRDS advances *useq* to the *seq* number of the next unacknowledged frame in the retransmission buffer (if any). This allows the MRDC to detect frames that exhausted its retransmission limit and flush the blocked frames from the reorder buffer.

The MRDC uses the source address in the MAC header and the *seq* value in the CTX header to identify the frames that belong to the same network-layer packet. When the MRDC receives at least 2 corrupt data frames that correspond to the same packet, it attempts frame combining on the payload part of the data frame. Since it is important that the MRDC correctly identifies the frames that belong to the same packet, RFA uses a 4-byte CRC to protect the MAC and CTX header. If either the MAC or the CTX header is corrupted, the MRDC drops the entire frame.

The MRD-ACK packet contains a 2-byte "magic" value that is used to distinguish the MRD-ACK packet from other downlink data payload,[9] a 1-byte sequence number, and an N-bit bit vector to indicate the success or failures of up to N consecutive frames. The sequence number is the *seq* value of the first data frame in the bit vector being acknowledged. The MRDS uses the link-layer data frame checksum to detect errors in the MRD-ACK packet.

The size of the MRD-ACK payload is small (25 bytes in our implementation). Thus, its overhead is dominated by the preamble and header associated with the 802.11 frame. We can potentially decrease overhead further by piggybacking MRD-ACK packets on data frames being transmitted in the same direction.

Our RFA implementation allows the MRDC to delay ACK transmissions in terms of the number of successive transmissions made by the MRDS. Thus, MRDC can delay an ACK either by a timeout of length equal to D packet transmission times or by counting D packet transmissions from the MRDS. Delaying ACKs by counting packets removes the requirement for sub-millisecond-granularity timers and allows the MRDC to be implemented in user space. Note that retransmitted frames are counted as a transmission while extra frames that are simultaneously received by different MRD radios should not be counted. Because both types of frames have identical *seq* values, the MRDC uses the *ntx* value to distinguish the retransmitted frames.

The MRDC sends MRD-ACKs to the MRDS via the active radio (i.e., the AP with which the WLAN client is associated for MRDS running in the WLAN clients). The MRDC may

also independently use fine-grained path selection [28] to choose the most reliable diversity radio for transmitting the MRD-ACK packet to the WLAN client.

7 Evaluation

We conducted several experiments to evaluate the performance of MRD under different conditions. We divide the presentation of the results into two categories, *HIVAR* and *LOVAR*, based on whether the WLAN client was experiencing a high or low degree of channel variability during the experiment. To create a high channel variability environment in HIVAR, we use a client transmitter that is set in motion during the experiment, while we use a stationary transmitter in LOVAR. Figure 8 illustrates the location of our APs and client in our HIVAR experiments. Due to space constraints, we omit the results for LOVAR, which are presented in [27]. We present the results of our HIVAR experiments, which includes performance evaluation on co-located radios and TCP that have not been previously presented.

7.1 Setup

We chose to conduct experiments in 802.11a mode to avoid interfering traffic from the production 802.11 WLAN in our lab. In all our experiments, we configure one of the AP receivers (R1 or R2) to be an active AP running in *Master* mode. We configure the other AP receiver to run passively in *Monitor* mode. We configure the client sender C to run in 802.11 *Managed* mode. We run the MRDS on the WLAN client to evaluate the performance for upstream traffic.

In all of the experiments, we set a maximum retransmission limit of 7 (one initial transmission plus up to seven retransmissions). The MRD experiments used a MRD-ACK delay of $D = 8$ packet transmissions, a sender buffer size of $N = 64$ packets, and a retransmission timeout of $T_s = 90$ ms. We pick $B = 256$ bytes ($\therefore N_B = 6$), such that the maximum
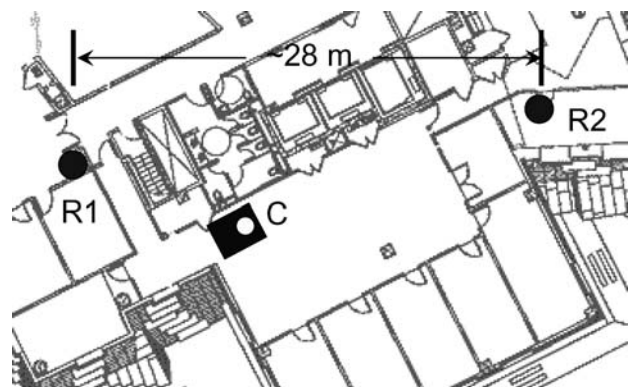

Fig. 8 Setup for the HIVAR experiments. R1 and R2 are stationary receivers. C is a laptop transmitter client that was carried by a walking person who covered a 1.5 m × 2 m area during the experiments

---

[9] Instead of using "magic", we should label the MRD-ACK with a unique value in the Ethernet `type` field [36]. We used the magic value in our implementation to facilitate logging using standard tools like `tcpdump` [2] during our experiments.

processing time to search through 2^{N_B} block combinations is less than S/r, where S is the transmitted frame size and r is the bit-rate. Bounding B in this way helps prevent the processing queue at the MRDC from building up.

In each experiment, the WLAN client sends 100,000 1472-byte UDP packets as fast as possible to saturate the wireless channel. We repeat each experiment for five trials. To help ensure each trial begins with fresh states, we re-load the wireless interface driver in between trials. On the first transmission of each packet, we insert a timestamp into the frame's payload. The timestamp remains unchanged on frame retransmissions. The timestamp allows us to measure and compare the packet delivery delay between MRD and the single radio communication schemes. Also, the payload of the packet contains a known bit pattern so that we can post-process the trace to analyze the probability of frame combining failure p_f as a function of different block sizes B.

Each MRD experiment involves two sub-experiments: in the first set (MRD-R1), we configure R1 to be the active AP with which the client associates and R2 to be the passive AP. In the second set (MRD-R2), R2 is active and associates with the client. We compared the performance using different active APs because the MRDS schedules retransmissions based on the link-layer feedback from the active AP.

As mentioned in Section 6, performing software-based retransmissions in the driver effectively disables exponential backoff in the wireless interfaces' firmware. To make a fair performance comparison between communication schemes, we used software-based retransmissions (and thus, disabling exponential backoff) in all of our experiments, including the single radio communication schemes. We discuss how disabling exponential backoff might affect our evaluation results in Section 8.

Because wireless communication is sensitive to the physical environment, we do not claim that the results of the experiments presented here are exhaustive and representative of *all* situations. Our main objectives are to conduct a set of experiments to illustrate the performance gains that MRD can achieve in the implemented system under a *real* environment

with different degrees of channel variability, and to analyze the properties of the MRD system in depth.

7.2 Throughput

We define throughput to be the sum of the payload bits from unique frames received divided by the time elapsed between the first and last frame receptions. Note that the throughput metric accounts for the overhead of the CTX header, MRD-ACK transmissions, and all the processing delay associated with MRD.

The average throughput over five trials for the single radio experiments R1 and R2 were 8.25 Mbps and 6.42 Mbps, which are far below 802.11a's theoretical maximum UDP throughput of 31 Mbps. The high channel variability caused by mobility and distance in our HIVAR experiments has significantly reduced throughput for the single radio communication schemes. Despite the harsh channel conditions, MRD-R1 and MRD-R2 maintained an average throughput of 18.7 Mbps and 18.36 Mbps respectively, which constitute improvements of $2.27\times$ and $2.23\times$ over R1 (and even more over R2). The gains of MRD indirectly confirms that path diversity exists in our experiment.

Moreover, the throughput of both MRD experiments are higher than the sum of the throughput values from both single-radio experiments. Hence, the results suggest that MRD could achieve a higher throughput than a scheme that aggregated the bandwidth of two radios to transmit data over orthogonal radio frequencies. Another words, our results show that MRD *can* outperform a system that uses roughly twice the wireless bandwidth as MRD!

We plot the throughput distribution of the one-second non-overlapping window samples in Fig. 9(a). For R1 and R2, 80% of the samples are between 4–10 Mbps and fewer than 10% of the samples achieved a throughput more than 15 Mbps. In contrast, MRD achieves a throughput greater than 15 Mbps for more than 85% of the samples. These results suggest that *even* if we allow the WLAN client for the
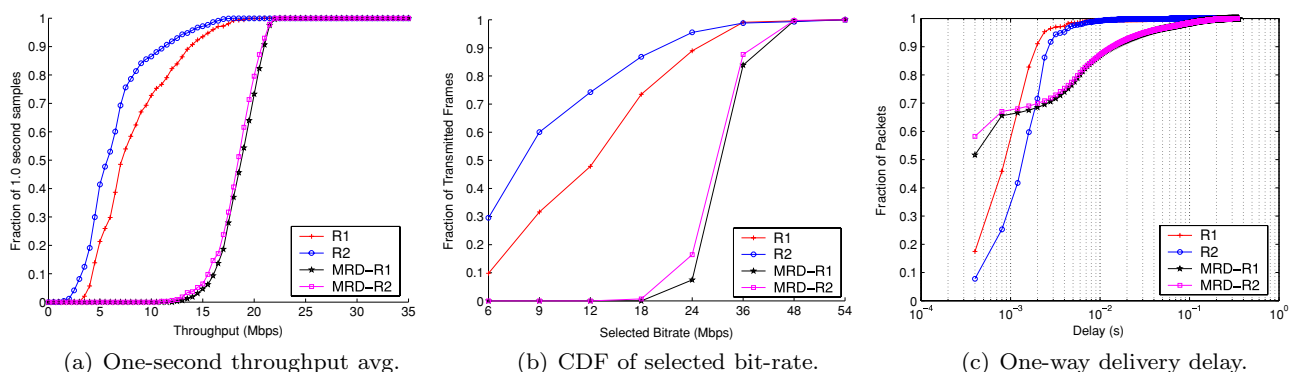

(a) One-second throughput avg.   (b) CDF of selected bit-rate.   (c) One-way delivery delay.

Fig. 9 HIVAR Experiment Analysis. Leftmost: Distribution of throughput averaged over non-overlapping one-second window samples. Center: Distribution of selected bit-rate for each transmission. Right: Delay above the minimum one-way packet delivery time

non-MRD schemes to perform handoffs every second, the average throughput will remain well below 15 Mbps.

Both MRD-R1 and MRD-R2 achieved similar throughput results. This suggests that the performance of MRD is relatively insensitive to the choice of active AP, even when there is a significant difference in link quality between the two APs.

7.3 Source of improvement

The large throughput improvement comes from the reduction in frame loss rate achieved by MRD. Table 2 summarizes the statistics of the raw frame loss rate (*FLR*) observed at the active AP in each sub-experiment and the ratio of the lost frames that were recovered (frame recovery rate, *FRR*) by MRD. The active APs in both sub-experiments suffered a raw *FLR* of about 35% and 39% but MRD was able to recover 50% and 57% of them, respectively.

The HIVAR experiments used the modified autorate algorithm as described in Section 5. Because MRD was able to conceal a large number of losses from the rate adaptation algorithm, the sender was able to maintain a high bit-rate throughout both sub-experiments, as depicted in Fig. 9(b), where over 90% of the frames were transmitted at a bit-rate of 24 Mbps or higher. In contrast, the single radio communication schemes suffers a high loss rate at the high bit-rates. Consequently, these schemes operate at low bit-rates. Actually, the selected bit-rates in R1 and R2 are spread across several of the low bit-rates due to the high degree of channel variability experienced by the client.

These results highlight the importance of MRDCALL-BACK(). If the procedure were not added to the autorate algorithm in MRD, the link-layer frame losses observed at the active AP would have been exposed to the autorate algorithm, causing MRD's to operate at the same low bit-rates as $R1$ and $R2$ in Fig. 9(b).

We decompose the recovered frames into frames recovered by soft selection (FRR_{SS}) and block-based combining (FRR_{FC}). Thus, $FRR = FRR_{SS} + FRR_{FC}$. Our results show that 85% and 90% of the gains in MRD-R1 and MRD-R2 were achieved by soft selection (i.e., those frames that were received correctly by the passive AP but not by the active one).

There are two possible explanations for the relatively small fraction of frames recovered by frame combining: (i)

there were few opportunities for running the packet combining either because most of the transmissions were already corrected by soft selection or because the MRDC did not collect enough valid corrupt frames (due to corrupt headers, etc.) to perform the combining; or (ii) there were many frame combining attempts but most of them failed to recover the correct frame.

We analyzed the number of successful and failed frame combining attempts. The total number of frame combining attempts was high, constituting 34% and 26% of the total number of frames that were not successfully received by the active AP in MRD-R1 and MRD-R2. Although there were many opportunities for error recovery with frame combining, about 80% of those attempts failed to correct the errors in the transmitted frame in both sub-experiments.

One cause for the high failure rate is the low number of block subdivisions in a frame in our implementation ($N_B = 6$). We post-processed the data trace of our experiments to analyze how p_f varies with other values for N_B and plot the results in Fig. 10(a).[10] The plot shows that p_f drops as N_B increases, which is consistent with the analytic model for burst bit-error channels that we developed in Section 3. For example, p_f drops from 80% to 60% when $N_B = 91$ (i.e., $B = 16$ bytes).

As discussed in Section 3, increasing N_B can potentially increase Δ, the number of differing blocks between two frames. To avoid overloading the MRDC, we may need to abort the frame combining operations for frames received with a large Δ. Thus, a high Δ for a large fraction of combining attempts can offset the performance gain from increasing N_B. Figure 10 plots the distribution of the number of unmatched blocks (Δ_{succ}) for the successfully combined frames at various N_B. For $N_B \leqslant 91$, the 75th percentile Δ_{succ} value are much smaller than N_B (e.g., for $N_B = 91$, the 75th percentile of Δ_{succ} is 10).[11] This suggests that we could improve the performance of frame combining by re-running our experiments with a larger N_B value.

Table 2 Frame loss and frame recovery rates of the high channel variability experiments

Experiment	*FLR*	*FRR*	FRR_{SS}	FRR_{FC}
MRD-R1	0.345	0.497	0.423	0.073
MRD-R2	0.391	0.573	0.515	0.058

---

[10] Recall that p_f excludes those frames that are successfully delivered by soft selection (Section 3.1). While the majority of frame combining attempts were performed for corrupt frames that were simultaneously received by the APs, a significant fraction of the frame combining attempts were performed with retransmitted frames. For simplicity, we excluded the retransmitted frames in our post processing analysis. Nonetheless, our results should remain representative because the retransmitted frames should have an independent bit error behavior similar to the simultaneously received frames.

[11] Performing $2^{\Delta} = 2^{10}$ frame combining checksum operations for a 1500-byte packet takes about four milliseconds on a 3.2 GHz Pentium IV PC. The processing time is rather large and may cause the processing queue to build up at the MRDC. However, it should be possible to reduce the processing time substantially by using an incremental CRC update algorithm [12, 34] or using specialized hardware to perform the CRC calculation.

(a) Failure rate.

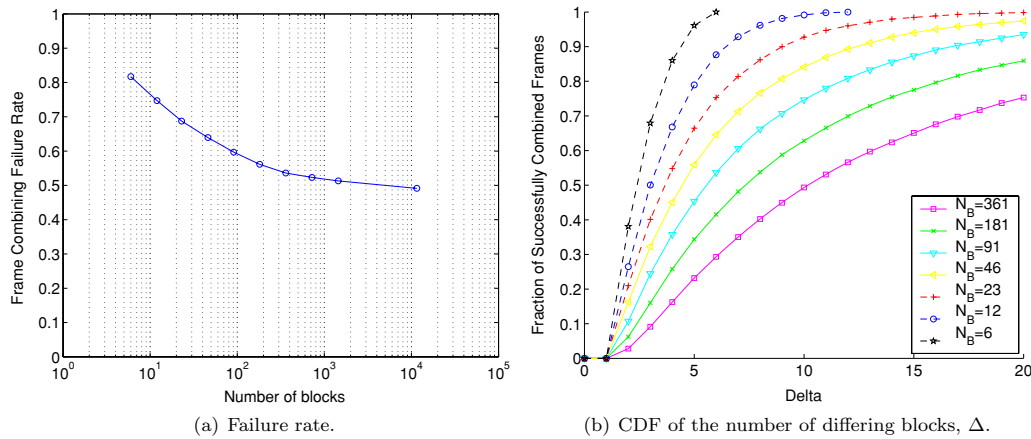(b) CDF of the number of differing blocks, Δ.

Fig. 10 Trace-driven simulation of p_f and Δ for various values of N_B in the HIVAR MRD-R1 experiments

Finally, the relatively low overhead of RFA allows MRD to achieve high gains. The number of MRD-ACKs transmitted constitute fewer than 7.5% of the total number of transmitted packets and fewer than 0.1% of the total number of transmitted bytes. The overhead of inserting an extra 7-byte CTX header to the 1500-byte packet payload is also negligible.

7.4 Delay analysis

A number of compelling wireless applications such as telephony and video streaming require a relatively low packet delivery delay not exceeding 100–150 ms [21]. We analyze MRD's delay performance here.

As described previously, we insert a timestamp in the payload of a packet's first transmission attempt to measure the one-way packet delivery delay. Because it is difficult to synchronize PC clocks to within a few tens of microseconds,[12] we do not measure the absolute packet delivery delay. Instead, we measure the delay jitter above the minimum one-way packet delivery time d_i for packet i, which does not require clock synchronization between the sender and the receiver. Let s_i and r_i be the start and receive timestamps associated with packet i for all $0 < i < 100,000$ packets transmitted in an experiment. Then $d_i = r_i - s_i - \min_i(r_i - s_i)$.

We also applied a piecewise linear regression algorithm [30] to remove clock skew between the sender and the receiver (we measured clock drifts on the order of 50 microseconds per second). Note that we can compute the one-way packet delivery delay by adding $\min_i(r_i - s_i)$, which includes the nominal transmission time and processing delay. In practice, this number is less than one millisecond. We will ignore this minor adjustment and use the terms "delay jitter" and "delay" interchangeably.

Figure 9(c) shows the one-way delay distribution for our HIVAR experiments. The MRD median delay is below 1 ms and has 25% more packets delivered than R1 and R2. The low median delay is due to its ability to maintain a high bit-rate throughout the experiments. However, about 35% of the packets in MRD were delivered with a significantly higher delay than R1 and R2. Nonetheless, MRD was able to deliver 95% of the packets within a delay of 35 ms, which is well below the delay bound of 150 ms that can be tolerated by telephony and video applications.

We attribute the increased packet delivery delay in MRD to the fact that there were a significant number of frames that required retransmissions because our rate adaptation algorithm uses a set of aggressive minimum delivery thresholds to improve throughput (Section 5). In the design of the MRDC, we assumed an in-order packet delivery service and added a re-order buffer at the MRDC (Section 4.3). Whenever a retransmission is required, the reorder buffer blocks subsequent packets from being forwarded and increases packet delivery delay for all of them.

Another source of delay comes from the losses of MRD-ACKs on the reverse channel, which delays the trigger to retransmit a packet. Also, the user space implementation of the MRDC is inefficient as interrupts and user space buffering can add delays in generating and sending MRD-ACKs.

7.5 Performance of co-located radios

We measure the performance of MRD for the case when the active and passive radios are co-located at the same site with each radio operating in the same radio frequency. This scenario is roughly equivalent to running MRD in the downlink direction, where the MRD radios are co-located on the wireless client. We also compare our results with those obtained with MRD radios that are separated over a large distance, and show the benefits of realizing diversity gains in the wide-area.
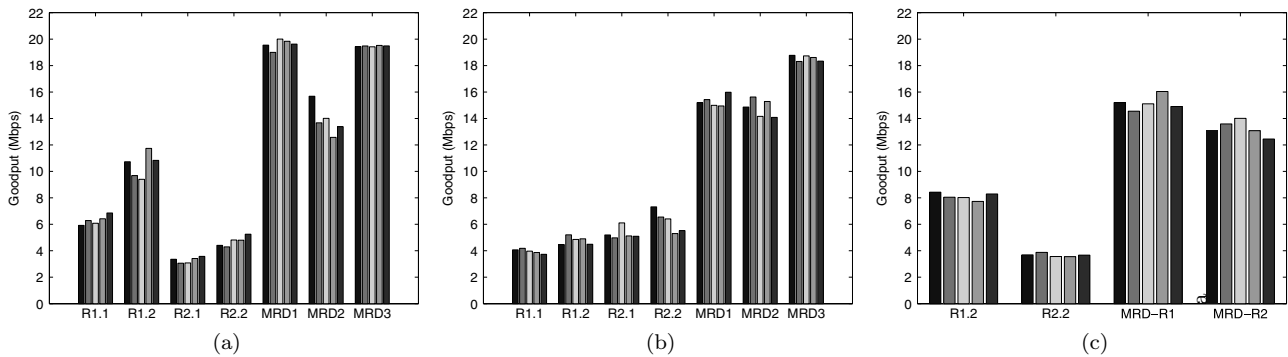
---

[12] We require the fine clock synchronization granularity because the nominal transmission time of 802.11a at high bit-rates is less than 0.5 millisecond.

Fig. 11 Left: Performance comparisons between co-located MRD radios and widely separated MRD radios. Each color bar represents the results of one experiment trial. Center: The same performance compar-ison repeated at different transmitter location. Right: Measured TCP throughput under various schemes

We use the same setup as in Section 7.1 and install one additional radio at each access point R1 and R2. The antennas of the co-located radios are placed at about 50 cm apart. We repeated the HIVAR experiments for the single radio schemes for the first radio at R1 (R1.1), and for the second radio at R1 (R1.2). Similarly, we repeated the single radio schemes for each of the two radios at R2 (labeled respectively as R2.1 and R2.2). We ran three HIVAR MRD experiments: MRD1 uses the co-located radios at R1, with R1.2 being the active radio, MRD2 uses the radios at R2, with R2.2 being active and MRD3 uses radios R1.2 and R2.2 at R1 and R2 respectively, with R1.2 being the active radio. The active radios were selected on the basis that they have the better link quality between the two radios.

Figure 11(a) shows the measured throughput of our experiments. Each experiment is repeated five times with the result of each trial plotted on a different color bar. R1.1 and R2.1 were the same radios that were used in the previous HIVAR experiments, but we measured a much lower average throughput of 6.3 Mbps and 3.3 Mbps for R1.1 and R2.1, than throughputs of 8.25 Mbps and 6.42 Mbps measured in the previous experiments. One possible cause for the difference is that the new set of measurements are conducted five months later than the previous ones and the furniture and obstacles in the surrounding environment changed in the meantime. Interestingly, the average throughput of R1.2 is about 1.66× greater than R1.1, even though the two radios are only 50 cm apart. These observations show how unpredictable wireless performance can be in an indoor environment.

Figure 11(a) shows that the MRD1, MRD2, and MRD3 schemes achieve average throughput of 19.6 Mbps, 13.9 Mbps, and 19.5 Mbps respectively, representing an improvement between from 1.88× to 2.9× over their non-MRD counterpart. Even though the MRD radios are placed in close proximity, MRD1 achieved the best result. Indeed, the correlation of signal envelopes between two closely-spaced antennas is around a quarter wavelength [32]. This corresponds to less than a few centimeters at the GHz frequencies. Thus, two

radios that are separated by about 50 cm are quite uncorrelated and would exhibit high diversity gains.

MRD2 underperforms both MRD1 and MRD3, because both radios at R2 are relatively far away and receive relatively weaker signals from the laptop transmitter. Thus, MRD2 illustrates a case where co-located radios can diminish the gain of MRD. When the MRD radios are co-located, they tend to share similar levels of path loss to the transmitter. Even though the instantaneous losses are uncorrelated, the average loss rates at each radio becomes increasingly correlated with distance, which eventually cancels out the diversity gains in MRD.

In contrast, MRD3 achieves almost the same performance as MRD1, even though the link quality for the passive radio (R2.2) in MRD3 is much lower than the passive radio (R1.1) in MRD1. One theory that explains this result is that the wide separation distance between the MRD radios reduces the average path loss correlation to each receiver, i.e., as the mobile laptop transmitter moves from one end of the test area to another, the average received signal strength might become weaker to one of the radio but stronger for another. Together, the wide-area MRD radios compliment one another and provide better overall signal reception coverage for the mobile transmitter.

To test this theory, we shifted the laptop's movement area by about one meter towards R2 and repeated our HIVAR experiments. We plot the measured throughputs in Fig. 11(b). Because the average distance to R2 has reduced, we observe an increased average throughput of 5.30 Mbps and 6.22 Mbps for R2.1 and R2.2. In contrast, R1.1 and R1.2 suffered a large throughput reduction to 3.96 Mbps and 4.78 Mbps. The reduction is especially drastic for R1.2, perhaps due to the non-line of sight signal propagation around the the hallway between the laptop and R1 (Fig. 8).

We observe similar trend for the MRD1 and MRD2 experiments. Compared to the previous experiment, MRD1's throughput reduced to 15.3 Mbps while MRD2's increased to 14.8 Mbps. On the other hand, MRD3 maintains a high

throughput and show only a small throughput decrease. MRD3 clocked a throughput of 18.6 Mbps, which is a 3× improvement over R2.2 and within 95% of the measured throughput in the original test area. These results suggest that the wide-area MRD radios can provide better overall reception coverage and maintain higher throughput than the co-located MRD radios in our experiments.

7.6 TCP performance

Although our experiments show that MRD achieves high UDP throughput gains, Section 7.4 discusses how MRD can introduce somewhat greater variation in packet delivery delay. Such effects could adversely affect TCP's performance. We conducted experiments to test if TCP performs well on MRD.

We ran the HIVAR experiments, using TCP to transmit about 72.4 MB of data from the mobile laptop and measured the average TCP throughput for two non-MRD schemes, R1.2 and R2.2, and two MRD schemes, MRD-R1 and MRD-R2. In MRD-R1, we configure the R1.2 and R2.2 radios to be the active and passive MRD radios respectively. In MRD-R2, we use the same radios but swap their active and passive roles. Note that our experiments run MRD only in the uplink direction. The TCP receiver runs on the same machine as the MRDC and uses a single radio (i.e., the active radio) to send TCP acknowledgment packets (TCP-ACKs) to the laptop.

In all of the TCP experiments, the laptop transmitter moves within the original test area as illustrated in Fig. 8. We observe that the single radio R1.2 and R2.2 experiments transmitted at an average throughput of 8.10 Mbps and 3.67 Mbps. The results correspond to about 78% of the throughput in the UDP experiments. The decreased throughput is not surprising given the overhead and congestion-controlled behavior of TCP.

MRD-R1 and MRD-R2 clocked an average throughput of 15.2 Mbps and 13.2 Mbps, which translates to about an 1.88× and 1.63× improvement over R1.2. Like the single-radio experiments, MRD-R1 achieves 78% of the throughput in the corresponding UDP experiment (MRD3). Because MRD-R1 achieves about the same proportion of UDP throughput as the single-radio TCP experiments, we believe that TCP remains largely unaffected by the delay variations and other link-level interactions in MRD.

Compared to MRD-R1, MRD-R2 achieves a lower proportion (68%) of MRD3's throughput. We have not analyzed our traces to determine the exact cause for the reduced gain but the link condition between the laptop and R2.2 is evidently poor. As a result, the TCP-ACKs could have suffered increased delay and losses in the reverse direction, impacting the sending rate in the forward direction.

8 Discussion

We discuss various implications that a MRD system has on rate adaptation, capacity, and contention control in wireless LANs.

8.1 Rate Adaptation

The conventional wisdom of managing link quality in WLANs is to have the clients adapt to the channel conditions (i.e., adapt the bit-rate) before changing to an alternate link (e.g., AP) with a better channel quality. MRD can be viewed as taking the opposite approach, where the clients use multiple links simultaneously before changing their bit-rate to adapt to the underlying diversified channel.

Our experimental results suggest that, with MRD, even a simple rate adaptation algorithm, such as the one based on MADWiFi, can perform well in different environments. In [27], we observed a large performance difference between the HIVAR and LOVAR experiments in the non-MRD schemes. We believe that the large performance difference is attributed not only to the increased frame loss rates observed at the individual APs, but also to the sub-optimal bit-rates that might have been chosen by the MADWiFi autorate algorithm in the high channel variability environment. (In Section 5, we tuned the algorithm to work well with multiple radios and frame combining, but did not alter the fundamental mechanisms used in the algorithm.)

In fact, we can use the results from the previous section to show that there is room for improvement in the rate adaptation algorithm. Table 2 and Fig. 9(b) show that the frame loss rate to the active AP in MRD-R1 was 35% and that MRD-R1 selected a bit-rate of at least 24 Mbps over 90% of the time. Multiplying $1 - FLR$ with the the effective throughput of the 24 Mbps (17.8 Mbps) bit-rate yields 11.6 Mbps. Thus, we could have fixed the bit-rate to 24 Mbps for the non-MRD HIVAR experiment ($R1$) to improve the performance by 1.4× over the MADWiFi autorate algorithm, which achieved 8.25 Mbps. (Although the improvement is significant, it is not as great as MRD-R1, which achieved a 2.3× improvement at 18.7 Mbps.)

We are not suggesting that a fixed bit-rate should be used for non-MRD wireless links operating in a channel with high variability: selecting an optimal fixed bit-rate for such a channel still requires an adaptive algorithm. Rather, our intent is to use the example to motivate the following open questions: (1) Could other existing autorate schemes (e.g., RBAR [17], AARF [22], MiSer [31], OAR [33], SampleRate [10]) be used to improve performance of the non-MRD schemes in our HIVAR experiments? (2) Can we design an autorate algorithm for a non-MRD WLAN that performs well under a variety of channel conditions in a real environment? These are open questions, but we have demonstrated—using real-world

experiments—that MRD can use a simple rate adaptation algorithm to produce good performance under different and difficult channel conditions, and that with MRD, the need for a finely tuned rate adapatation algorithm is not as important as with schemes that use single-radio terminals.

Finally, we should consider developing a rate adaptation scheme that can help reduce packet delivery delay for MRD. Because retransmissions in MRD requires higher delay than conventional scheme, as shown in Section 7.4, we should modify the rate adaptation algorithm (e.g., adjust the minimum delivery threshold) to reduce retransmissions. Although doing so might trade off throughput gains for reduced delays, we believe that it is possible to develop an algorithm that provides both througput gains and reduced delays in MRD because of MRD's fundamental ability to reduce frame loss rates and their variations.

8.2 Capacity

One may raise the question whether the overall capacity of a wireless network drops with MRD since an MRD system sacrifices the possibility of channel reuse at different APs for the sake of increased reliability for individual sessions. Let us consider a simple scenario with two terminals, T1 and T2 and two APs, R1 and R2. In the non-MRD system, each terminal is assigned to a single AP and transmit in orthogonal radio channels. In the MRD system, we equip R1 and R2 with multiple radios such that each can receive transmissions from T1 and T2 at the same time. Thus, we have two MRD sessions, T1-(R1,R2) and T2-(R1,R2) running simultaneously over different channels. In this case, it is clear that the MRD system has a higher capacity than the non-MRD system since it has two extra transmissions (T1-R2 and T2-R1) over the non-MRD system without extra cost or interference to the existing transmissions, T1-R1 and T2-R2.

The results are similar if we assume that all nodes operate in the same radio frequency and that the two pairs T1-R1 and T2-R2 are close to each other (i.e., adjacent cells) such that simultaneous transmissions from both terminals cause significant interference to each other. Then under any channel access scheme that avoids simultaneous transmissions (mutual interference) from the two transmitters (e.g., CSMA), the MRD system will have a higher capacity than the non-MRD system. Like the previous scenario, the MRD system here provides extra complementary transmissions (T1-R2 and T2-R1) to improve the reliability of the communication between the terminals and the APs.

However, the results are different if we allow T1-R1 and T2-R2 to transmit in different channels in the non-MRD system but constrain R1 and R2 to operate in the same channel

in the MRD system.[13] In this case, the total capacity for the non-MRD system is higher than the capacity of the MRD system because simutaneous transmissions are possible in the non-MRD system whereas only one terminal may transmit at a time in the MRD system due to the terminals' mutual interference.

Nonetheless, one can observe in Fig. 11(a) that the throughput of a single terminal in the MRD system is higher than the combined throughput of T1-R1 and T2-R2 for the non-MRD system. Assuming that the combined throughput of the single-radio experiments closely approximates the aggregate throughput of the simultaneous communications (T1-R1 and T2-R2) in the non-MRD system, our experimental results suggest that the MRD system can sometimes outperform the non-MRD system even though the capacity of the latter system is higher.

As discussed in the previous section, we believe that the reason for MRD's higher *achieved throughput* is the better utilization of the resources with the MRD system. In fact, MRD not only reduces the frame loss rate, but also dampens the fluctuations in the frame loss rate. When the channel parameters are more stable, the rate adaptation algorithm does a better job in exploiting the existing bandwidth in the system. Hence, even though the non-MRD system has a higher capacity, it may not be utilized efficiently due to more variable conditions in each channel.

In the general case of more than 2 terminal-AP pairs, the capacity analysis is fairly complex and is beyond the scope of this paper. However, based on the examples given in the previous paragraphs, we can conclude that if the number of channels is sufficiently high, MRD can increase the capacity of the network, since we can set extra connections between a terminal and an AP that are not directly paired, without causing any interference to the existing transmissions of the AP. Moreover, we illustrated an example in which MRD leads to a higher achieved throughput despite a lower raw capacity, because MRD provides less variable channel conditions that lead to better adaptiveness of the rate adaptation algorithm and better utilization of the wireless medium.

8.3 Link-layer contention control

As mentioned in Section 6, the MRDS needs to assume control over all retransmissions. Performing software-based retransmissions in the driver, however, also has the side effect of disabling the exponential backoff controlled by the firmware.

We acknowledge that the relative throughput improvement by MRD may be reduced when exponential backoff is

---

[13] This setup is a simplification of the following problem: When a network operator adds *single-radio* APs in a WLAN, is it better to run MRD by configuring them as passive radios or is it better create a new cell by configuring them as a regular AP?

enabled. That is because the link layer increases the back-off window whenever a client fails to successfully transmit a data frame to the target receiver (i.e., the active AP) at the link layer. In our current design, the link layer is oblivious to MRD. Even if the data frame is recovered through soft selection or block-based combining, the link layer may not reduce the contention window (which is what CSMA does when the link-layer transmission succeeds). Consequently, the backoff window may increase unnecessarily and reduce MRD's performance.

We can alleviate the problem by creating an interface that allows MRD to inform the link-layer backoff mechanism about the results of frame recovery at the MRDC. Designing a medium access control algorithm that can adapt to MRD's error recovery results is an interesting open problem. As an alternative, we can adopt some of the recently proposed channel access methods that do not rely on link-layer acknowledgments but adjust the contention window size based on the measured idle channel time [16, 37].

Despite the above caveat, MRD effectively reduces frame losses and the total number of transmissions required to deliver a packet, without increasing the nominal frame transmission time as in other existing approaches like using lowering data rates or employing forward error correction.

9 Related work

The idea of coordinating multiple radios in WLANs has recently received considerable attention. The authors in [9] proposed to embed multiple radios on a single device for better energy and mobility management, capacity enhancement, and avoiding channel failures. A system that uses fine-grained path selection (FGPS) that switches transmissions from among a set of nearby APs was demonstrated to effectively reduce path dependent losses in WLANs [28] and to improve the quality of video streaming applications [26]. FGPS takes advantage of path diversity at the *transmit side* of the system. MRD compliments FGPS to reap the benefit of path diversity at the *receive side* of the system.

Diversity reception is a common technique used to mitigate the effects of fading, and interference in wireless systems. Almost all WLAN devices have embedded more than one antenna that gets selected based on packet loss rates. Recently, the IEEE incorporated a more advanced antenna diversity technique Multiple-Input Multiple-Output (MIMO) [29] into the physical layer specifications of their next generation WLAN devices known as 802.11n [41]. In general, this class of techniques, known as *microdiversity*, are tightly integrated with the physical layer and mostly help in mitigating path-dependent effects localized at one receiver. In contrast, MRD is a solution that may be readily deployed today in any 802.11 system by just changing the software. Furthermore, MRD

WLANs operate above the physical layer and may be used to collect data frames received by radios distributed across different access points at different locations to realize diversity gains at the macro level, which can yield significant performance improvement as shown in Section 7.5. Thus, we believe MRD and MIMO can compliment one another: a WLAN operator can build a MRD WLAN using 802.11n hardware to exploit path diversity locally at the receiver and remotely over the wide-area.

Code Division Multiple Access (CDMA) cellular phone networks have long used "macrodiversity" to improve performance and to provide seamless handoff between base stations [32]. This idea is later applied to combine frames received from adjacent access points to improve uplink WLAN performance in the same way as MRD. [23] presents simulated results based on a capture model but ignores protocol level issues such as ARQ. The contributions of [14, 24, 39] focus on theoretical performance analysis, with [39] presenting results in the context of a WLAN based on Bluetooth [11] radios. In contrast, our contributions lie in the design of a macrodiversity system that works well in CSMA-based WLANs and in conducting a performance study of a fully implemented receiver macrodiversity system on a real testbed.

The idea of recovering a frame by combining it with a retransmitted version was first proposed in [35] and then further analyzed in [14, 15]. Hybrid ARQ is an extension of this technique, which combines forward error correction (FEC) and retransmission to recover unsuccessful transmissions [25]. Although numerous hybrid ARQ schemes are available, we chose block-based combining because it has the advantage that (1) there is no encoding and it inserts no extra FEC bits into the frame, (2) it uses hard decision (i.e., it performs correction using only the received data bits without requiring extra information from the physical layer), and consequently (3) the algorithm is easy to implement. A scheme proposed in [8] uses collaborative decoding to improve link reliability. The scheme is complex and requires the receivers to exchange soft decision estimates of each data symbol, which is not accessible from any wireless device on market today.

A proposal that uses 802.11's request-to-send(RTS)/clear-to-send(CTS) control packets to convey the results of packet combining is outlined in [14]. Because RTS/CTS is required for every transmission, the proposed method (which was not implemented and experimentally evaluated) will produce much higher overhead than our RFA protocol.

Like MRD, multi-user diversity [20] and medium-access diversity [19] also exploit the fact that losses at different receivers occur independently. In both techniques, an AP has a queue of packets destined for different clients and attempts to improve network performance by scheduling transmissions to the client receiver that has the best channel condition in a given moment. In contrast to MRD, the technique requires explicit receiver selection and channel quality feedback from

each receiver. These requirements are necessary if the receivers are not inter-connected by a high bandwidth back-channel that MRD relies upon.

10 Conclusion

MRD uses wireless path diversity to improve loss resilience in wireless local area networks. It coordinates wireless receptions among multiple radios—either co-located on the same device or distributed across different access points in the WLAN infrastructure—to increase loss resilience against path-dependent corruptions in the wireless medium. Using multiple radios, MRD performs frame combining, which attempts to correct bit errors by combining corrupt copies of data frames received by each radio in our system. Because losses are often independent among different receivers, MRD is able to achieve significant improvement in loss rates.

Our experiments in an in-building testbed using commodity PCs and 802.11a/b/g wireless interfaces demonstrate throughput gains of up to $3\times$ that of single radio communication schemes, with the corresponding one-way delay bounded to 35 ms for 95% of the delivered packets.

From the experience we gathered in building and evaluating MRD, we discovered a number of performance optimizations such as marking packets for low-latency and out-of-order delivery, and sharing MRD feedback with the link-layer to improve rate adaptation and contention window adjustments. We plan to pursue to design and integrate these optimizations to further improve the performance of MRD in the future.

References

1. Madwifi: Multiband Atheros Driver for WiFi. http://madwifi.sourceforge.net/.
2. tcpdump/libpcap. http://www.tcpdump.org.
3. Engim product overview. (2003) http://www.engim.com/products.html
4. IEEE P802.11i/D10.0. Medium Access Control (MAC) Security Enhancements, April 2004.
5. Madwifi mailing list archive. (Feb. 2005) http://news.gmane.org/gmane.linux.drivers.madwifi.devel.
6. IEEE 802.11b/d3.0 Wireless LAN Medium Access Control (MAC) and Physical Layer (PHY) Specification (Aug. 1999).
7. *IEEE Standards for Local and Metropolitan Area Networks: Standard for Port Based Network Access Control* (Oct. 2001).
8. A. Avudainayagam, J. Shea, T. Wong, and X. Li, "Reliability exchange schemes for iterative packet combining in distributed arrays," in: *Proc. of IEEE WCNC*, New Orleans, LA (March 2003) pp. 832–837.
9. P. Bahl, A. Adya, J. Padhye, and A. Wolman, "Reconsidering wireless systems with multiple radios," *ACM CCR* (Oct. 2004) pp. 39–46.
10. J. C. Bicket, "Bit-rate selection in wireless networks," Master's thesis, Massachusetts Intitute of Technology, Cambridge, MA, (Feb. 2005).
11. Specification of the bluetooth system (Dec. 1999). http://www.bluetooth.com/. Bluetooth Special Interest Group document.
12. F. Braun and M. Waldvogel, "Fast incremental CRC updates for IP over ATM networks," in: *Proc. of IEEE HPSR*, Dallas, TX (May 2001).
13. S. Chakraborty, E. Yli-Juuti, and M. Liinaharja, "An ARQ scheme with packet combining," *IEEE Communications Letters*, Vol. 2 (1998) pp. 200–202.
14. S. S. Chakraborty, M. Lilnaharja, and K. Ruttik, "Diversity and packet combining in rayleigh fading channels," *IEE Proceedings-Communications*, Vol. 152 (June 2005) pp. 353–356.
15. A.-G. A. Daraiseh and C. W. Baum, "Methods for packet combining in HARQ systems over bursty channels," *Mobile Networks and Applications*, Vol. 2 (1997) pp. 213–224.
16. M. Heusse, F. Rousseau, R. Guillier, and A. Duda, "Idle sense: An optimal access method for high throughput and fairness in rate diverse wireless LANs," in: *Proc. of SIGCOMM'05*, Philadelphia, PA (Aug. 2005) pp. 121–132.
17. G. Holland, N. H. Vaidya, and P. Bahl, "A rate-adaptive MAC protocol for multi-hop wireless networks," in: *Proc. of ACM MobiCom*, Rome, Italy (July 2001) pp. 236–251.
18. IEEE 802.11 Working Group. *Draft Supplement to International Standard for Information Exchange between Systems—LAN/MAN Specific Requirements*, Nov. 2001.
19. Z. Ji, Y. Yang, J. Zhou, M. Takai, and R. Bagrodia, "Exploiting medium access diversity in rate adaptive wireless LANs," in: *Proc. of ACM MobiCom*, Philadelphia, PA (Sept. 2004) pp. 345–359.
20. R. Knopp and P. A. Humblet, "Information capacity and power control in single-cell multiuser communications," in: *Proc. of IEEE ICC*, Seattle, WA (June 1995) pp. 331–335.
21. A. Kopsel and A. Wolisz, "Voice transmission in an IEEE 802.11 WLAN based access network," in: *Proc. of ACM WoWMoM*, Rome, Italy (July 2001) pp. 23–32.
22. M. Lacage, M. H. Manshaei, and T. Turietti, "IEEE 802.11 rate adaptation: A practical approach," in: *Proc. of ACM MSWiM*, Venezia, Italy (Oct. 2004) pp. 126–134.
23. V. C. M. Leung and A. W. Y. Au, "A wireless local area network employing distributed radio bridges," *Wireless Networks*, Vol. 2 (1996) pp. 97–107.
24. Y. Liang and S. S. Chakraborty, "ARQ and packet combining with post-reception selection diversity," in: *Proc. of IEEE VTC'04*, Los Angeles, CA (Sept. 2004).
25. S. Lin, D. Costello, and M. Miller, "Automatic-repeat-request error-control schemes," *IEEE Communications Magazine*, Vol. 22 (1984) pp. 5–17.
26. A. Miu, J. Apostolopoulos, W. T. Tan, and M. Trott, "Low-latency wireless video over 802.11 networks using path diversity," in: *Proc. of IEEE ICME*, Baltimore, MD, Vol. 2 (July 2003) pp. 441–444.
27. A. Miu, H. Balakrishnan, and C. E. Koksal, "Multi-radio diversity in wireless networks," in: *Proc. of ACM MobiCom*, Cologne, Germany (Sept. 2005).
28. A. Miu, G. Tan, H. Balakrishnan, and J. Apostolopoulos, "Divert: Fine-grained path selection for wireless LANs," in: *Proc. of ACM MobiSys*, Boston, MA (June 2004) pp. 203–216.
29. A. F. Molishch and M. Z. Win, "MIMO systems with antenna selection," *IEEE Microwave Magazine* (2004) pp. 46–56.

30. S. B. Moon, P. Skelly, and D. Towsley, "Estimation and removal of clock skew from network delay measurements," in: *Proc. of IEEE INFOCOM*, New York, NY, Vol. 1 (March 1999) pp. 227–234.

31. D. Qiao and S. Choi, "Goodput enhancement of IEEE 802.11a wireless LAN via link adaptation," in: *Proc. of IEEE ICC*, Helsinki, Finland, (June 2001) pp. 161–175.

32. T. S. Rappaport, *Wireless Communications*. Prentice Hall, Upper Saddle River, N.J. (1996).

33. B. Sadeghi, V. Kanodia, A. Sabharwal, and E. Knightly, "Opportunistic media access for multirate ad hoc networks," in: *Proc. of ACM MobiCom*, Atlanta, GA, (Sept. 2002) pp. 24–35.

34. J. Satran, D. Sheinwald, and I. Shimony, "Out of order incremental CRC computation," To appear: IEEE Trans. on Computers, 2005. `http://www.haifa.il.ibm.com/satran/ips/crc23feb2003.pdf`.

35. P. Sindhu, "Retransmission error control with memory," *IEEE Trans. on Communications*, Vol. 25 (1977) pp. 473–479.

36. R. W. Stevens, *TCP/IP Illustrated*. Addison-Wesley, Reading, MA, 1994.

37. G. Tan, "'Improving aggregate user utilities and providing fairness in multi-rate wireless LANs," PhD thesis, Massachusetts Institute of Technology, (Feb. 2006).

38. C. Tang and P. K. McKinley, "Modeling multicast packet losses in wireless LANs," Technical report, Computer Science and Engineering Department, Michigan State University (May 2003).

39. M. C. Valenti, "Improving uplink performance by macrodiversity combining packets from adjacent access points," in: *Proc. of IEEE WCNC*, New Orleans, LA (March 2003) pp. 636–641.

40. A. Willig, M. Kubisch, C. Hoene, and A. Wolisz, "Measurements of a wireless link in an industrial environment using an IEEE 802.11-compliant physical layer," *IEEE Trans. on Industrial Electronics*, Vol. 43 (2002) pp. 1265–1282.

41. J. M. Wilson, *The next generation of wireless LAN emerges with 802.11n*, Device Forge, August 2004. `http://www.deviceforge.com/articles/AT5096801417.html`
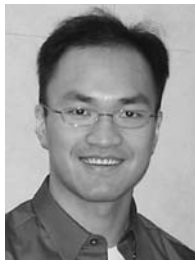
Allen Miu received his Ph.D. degree at the Massachusetts Institute of Technology in 2006 and is currently a wireless systems architect at Ruckus Wireless, Inc. He received his S.M. in Computer Science from MIT and a B.Sc. with highest honors in Electrical Engineering and Computer Science from the University of California at Berkeley. He previously worked onthe Cricket Indoor Location System and was a research intern at Microsoft Research, Redmond in 2000 and Hewlett-Packard Laboratories, Palo Alto in 2002. His research interests include wireless networks, location systems, mobile computing, and embedded systems.

Hari Balakrishnan is an Associate Professor in the EECS Department and a member of the Computer Science and Artificial Intelligence Laboratory (CSAIL) at MIT. His research interests is in the area of networked computer systems. In addition to many widely cited papers, several systems developed as part of his research are available in the public domain. He received a Ph.D. in Computer Science from the University of California at Berkeley in 1998 and a B.Tech. from the Indian Institute of Technology (Madras) in 1993. His honors include an Alfred P. Sloan Research Fellowship (2002), an NSF CAREER Award (2000), the ACM doctoral dissertation award for his work on reliable data transport over wireless networks (1998), and seven award-winning papers at various top conferences and journals, including the IEEE Communication Society's William R. Bennett Prize (2004). He has also received awards for excellence in teaching and research at MIT (Spira, Junior Bose, and Harold Edgerton faculty achievement awards).

C. Emre Koksal received his B.S. degree in Electrical Engineering from the Middle East Technical University, Ankara in 1996. He received his S.M. and Ph.D. degrees from MIT in Electrical Engineering and Computer Science in 1998 and 2002 respectively. He was a postdoctoral fellow in the Networks and Mobile Systems Group in the Computer Science and Artificial Intelligence Laboratory at MIT until 2003. Since then he has been a senior researcher jointly in the Laboratory for Computer Communications and the Laboratory for Information Theory at EPFL, Switzerland. His general areas of interest are wireless communications, computer networks, information theory, stochastic processes and financial economics. He also has a certificate on Financial Technology from the Sloan School of Management at MIT.